COBEM 2023 27TH INTERNATIONAL CONGRESS OF MECHANICAL ENGENEERING

ABCM Brazilian Society of Mechanical Sciences and Engineering
27th ABCM International Congress of Mechanical Engineering
December 04-08, 2023, Florianópolis-SC, Brazil

COB-2023-0425
AN INVESTIGATION OF THE PERFORMANCE OF TRISO FUEL AND MOLTEN FLUORIDE SALTS

Daniel de Souza Gomes
Instituto de Pesquisas Energéticas e Nucleares (IPEN / CNEN - SP), Av. Professor Lineu Prestes 2242, São Paulo,SP, Brazil.
dsgomes@ipen.br

Abstract. *Public opinion has reached a growing consensus that nuclear energy could be an inflection point for mitigating global warming and the shortage of natural resources in the future. The energy demand suffers a rapid increase and can duplicate itself up to 2035. Since 2002, Generation IV has researched at least six designs to substitute nuclear power plants with forty years of operation. Fluoride high-temperature reactor designed to use tri-structural fuel formed of graphite-matrix-coated particles with a mixture of lithium and beryllium fluorides as coolant, commonly called FLiBe. However, concisely, the heat transfer models applied to nuclear reactors depend on the Prandtl number correlated to coolant and usage conditions. A pebble-bed fluoride-salt-cooled high-temperature reactor, Mark-1, comprises a conceptual project developed at Berkeley in 2016. Then, it performs a theoretical analysis of the core reactor, where we review the thermal properties of fuel and coolant. It compares generation-IV reactor design analysis with options such as heavy liquid metals, coolants, molten salt reactors, and conventional fuels.*

Keywords: *Molten salt reactor, FHR, FliBe, FLiNaK, TRISO*

1. INTRODUCTION

Nuclear power is a valuable option for electric power generation since it produces no carbon emissions and is a well-established commercial technology (Krey et al., 2014). In the 1970s and 1980s, nuclear power units expanded significantly worldwide (Carrara, 2020). Because of the growth of renewable energy, government agencies have sponsored several programs for solar and wind that are driving the future of power generation (Cousse, 2021). After the turn of the millennium, there was a resurgence of interest in nuclear energy as a source of electricity. In 2021, about 60 power reactors were under construction in 15 countries, particularly China, India, and Russia. Nuclear units can take several building years, and the operational life of facilities is around 40 years. Currently, pressurized water reactors (PWRs) and boiling water reactors (BWRs) dominate electric generation scenarios, supplying over 10% of the world's electricity (Ho et al., 2019).

Today, 410 nuclear power reactors operate in 32 countries, with a capacity of about 368 GW (Pioro et al., 2023). Light-water reactors (LWRs) operate with uranium dioxide (UO_2), a solid fuel built during the third generation of reactors, and many have served for over 40 years. PWRs and BWRs operate with water coolant at temperatures around 275 °C and 283 °C, respectively, with high pressures of 15 MPa and 7 MPa and a thermal efficiency of less than 35%. (Fernández-Arias et al., 2020).

In 1946, the US Army Air Force began the Aircraft Nuclear Propulsion (ANP) program to enable supersonic long-range flight. The ANP and the preceding Nuclear Energy for the Propulsion of Aircraft (NEPA) plan had a cost of $24 billion until May 1951. However, it limited American uranium reserves in the 1950s. With fissionable U-235 and fertile U-238, natural uranium contains 99.28% U-238 and 0.72% U-235. The enrichment procedure was expensive and time-consuming, meaning that 140 tons of natural uranium were needed for every U-235 produced. Then, two researchers from Oak Ridge National Laboratory (ORNL), Eugene Wigner and Alvin Weinberg, proposed the Molten Salt Reactor (MSR). They presented the concept of liquid fuel using thorium to convert to the fissile isotope U-233 (MacPherson, 1985).

In 1954, carried out by the US Air Force, the Aircraft Reactor Experiment (ARE) was the initial prototype. The MSR showed a thermal power of 2.5 MW and operated in the thermal spectrum. MSR was the first reactor that used liquid fuel and coolant, using the molten sodium fluoride salt NaF-ZrF_4-UF_4 (53.09-40.73-6.18 mole%). Molten salt has a density of 416.5 kg/m^3, contains U-235, and uses beryllium oxide as a moderator. The ORNL built and operated the Molten Salt Reactor Experiment (MSRE) (Haubenreich et al., 1970). MSRE operated with alkali fluorides like lithium-beryllium fluoride (^{7}LiF-BeF_2) or FliBe between 1965 and 1969. MSRE was a test reactor at ORNL with an output of 7.4 MW using graphite as a moderator. In short, the Molten-Salt Reactor Program (MSRP), run by ORNL from 1958 to 1976, developed much of the molten salt technology (Singh et al., 2018). In 1968, three years later, it was the first reactor to operate on U-233. Since 2001, the Generation IV International Forum (GIF) has researched future nuclear designs. The GIF has representatives from 13 countries and comprises Euratom, representing 27 European Union members.

Since then, the GIF initiative has promoted research focused on six types of reactors for further international study and development. Summarily, Generation IV systems show four broad targets: sustainability, economics, safety and

reliability, physical protection, and proliferation risk (Zohuri, 2020; Schulenberg, 2022). Among the six candidates proposed in the GIF, the molten salt reactors show two main subclasses (Serp et al., 2014). Thus, the MSR concept provides advantages over other technologies. Among these benefits, it lists meltdown mitigation through passive cooling, negative temperature coefficients of reactivity, and operating near atmospheric pressure. The lowest parasitic neutron capture is essential for achieving negative void reactivity feedback. FLiBe is vital for liquid fuel because of its high potential to dissolve Th-232, Pu-239, and U-235. Besides, it has a melting and boiling point that should allow operation at a thermal limit of around 1000 °C. Further, fluoride high-temperature reactors (FHR) combine the operation with spherical fuels (Seifried et al., 2019). The GIF shows sodium fast reactors (SFRs) as an option because they allow high power densities.

Today, the MSRs permit operating with liquid or solid fuel to burn actinides and produce fissile fuels (breeding). High temperatures allow electricity generation and hydrogen production. These reactors have used Tri-Structural ISOtropic (TRISO) fuel (Elder and Allen, 2009; Satvat et al., 2021). Then, the long experience gained in high-temperature gas-cooled reactors (HTGRs) combined with the molten salts changed from helium's coolant to FliBe. The very high temperature reactors (VHTRs) used an iodine-sulfur method composed of three chemical reactions. Start with the Bunsen reaction, which produces sulfuric acid and hydrogen iodide when water, sulfur dioxide, and iodine react. Then, it followed the H_2SO_4 section and got the target iodidric acid (HI) and hydrogen gas. (Wang et al., 2021).

Besides, GIF promotes a closed fuel cycle that can reprocess burned fuel and partly reuse it. The remaining uranium, plutonium, and waste isotopes carry proliferation threats in closed fuel cycles. In 2011, the Chinese government started a liquid fluoride thorium reactor, the Thorium-Breeding Molten-Salt Reactor (TMSR). TMSR-LF1 operates with liquid fuel fluoride molten salt mixed with thorium and uranium (^{7}LiF-BeF_2-ThF_4-$^{233}UF_4$). The power generated is 2 MW and permits online reprocessing and refueling. TMSR shows a substantial neutron economy operating at atmospheric pressure. The second prototype is the TMSR-SD1 with 10 MWth using TRISO fuel with a diameter of 6 cm and FLiBe as coolant. China plans to change its thorium energy operations in 20–30 years (Xu et al., 2019).

In 2018, Kairos Power (KP) introduced the conceptual design of the KP-FHR, which generates 140 MW using TRISO fuel (Stavat, 2021). KP-FHR is a pebble bed with an enrichment of 19.75% U-235 and FLiBe as a coolant (Blandford et al., 2020). Chloride salts produce less tritium than fluoride salts. Startups have created various MSR designs, such as Moltex Energy, Elysium Industries, and TerraPower. Chloride salts like NaCl-UCl_3 became a reference to being a desirable carrier salt because of their high solubility power. Besides, fluoride salt has a high heat capacity, double sodium, and a thermal conductivity double that of water. This way, fluoride salts improve heat transfer with a high thermal efficiency of 42.5% compared with 40% in sodium reactors (Novak et al., 2021).

This research analyzes the TRISO fuel coupled with the molten salts, which shows better thermal performance at high temperatures. Molten salts such as fluoride, nitrate, chloride, and carbonate salts have been suggested for heat transfer, thermal energy storage, and nuclear applications involving several options. In this way, the physical properties of molten salts, such as melting point, thermal conductivity, specific heat capacity, enthalpy, and Gibbs free energy, are reviewed. They also involve a simple revision of the fluid properties, like the viscosity of molten salts. In addition, it analyzes the Reynolds number varying from 10000 to 50000 and the Prandtl number between 10 and 27, with implications.

2. MATERIAL AND METHODS

The prototype HTGR was the Peach Bottom Unit 1, which operated from 1966 to 1974 using helium as a coolant. In the 1980s, the US government established HTGR research and development plans. The Germans incorporated spherical fuel elements simultaneously with the core design, including ceramic-coated fuel particles. There are essential differences in the properties of refrigerants. Sodium coolant operates at 500 °C at 15 MPa. Fast gas reactors work with helium at 500 °C with 7.1 MPa for thermal and fast neutron spectra. Further, fluoride salts operate at 600 °C with 0.23 MPa. Table 1 lists a few properties of the fluoride salts, helium gas, and liquid sodium.

Table 1. Comparison of a few physical properties of the fluoride salts, helium gas, and sodium as coolants.

Physical properties	**He 7.5 MPa**	**Na (700 °C)**	**^{7}LiF-BeF_2 (66-34)**	**NaF-ZrF_4 (59.5-40.5)**	**^{7}LiF-NaF-KF (46.5-11.5-42)**	**^{7}LiF-ThF_4 (72-28)**
Weight (g/mol)	4	23	33.0	92.7	41.3	87.99
Melting point (°C)	-272.2°C	98	459	500	454	555
Boiling point(°C)	-268.93	883	1727	1350	1570	1674
Density (Kg/m^3)	3.8	845	1.994	2.8264	2.718	4470
Heat capacity (kJ/kgK)	5.19	1.27	2.414	1.161	1.151	1.05
Thermal conductivity (W/mK)	0.281	62	1.0	0.49	0.92	1.2
Viscosity (cp)	0.041	0.182	5.6	5.1	2.9	16.74

The intention to produce hydrogen needs the advantages offered by ceramic-coated particle fuel and the operation of FLiBE at high temperatures at low pressure. The High-Temperature Engineering Test Reactor (HTTR) comprises a gas-cooled reactor operating at an outlet temperature of 850°C to 950°C. HTTR shows a prismatic core design similar to the Chinese HTR-10, first implemented in Japan in 1991 (Suh et al., 2022). After German experience gained in gas-cooled reactors, South Africa developed the pebble bed modular reactor (PBMR) between 1994 and 2009 (Reitsma). The design resembled HTTR, adopting a pebble bed, helium cooling, and graphite moderation. Oak Ridge constructed the Advanced High-Temperature Reactor (AHTR) along the same line in 2006. Like the VHTR, the AHTR uses helium as a coolant and runs at 900 °C. Besides, the AHTR design supports coolants such as $^{7}LiF\text{-}BeF_2$, $NaF\text{-}BeF_2$, $LiF\text{-}NaF\text{-}KF$, and $NaF\text{-}ZrF_4$.

2.1 High-temperature reactors

The High-Temperature Reactor Dragon Project began operations in the United Kingdom at Winfrith in 1966. The Dragon prototype generated 2 MWe, starting a new fuel design: low-enriched coated-particle fuel, prismatic graphite, and helium as a coolant. With an inlet gas temperature of 350 °C and an outlet temperature of 750 °C, the mass flow is 10 kg/s at 2.03 MPa. The American initiative started with high-temperature reactors based on coated particles surrounded by pyrolytic carbon. During the 1960s, American HTRs emerged, such as Peach Bottom with 40 MWe in 1967 and Fort Saint-Vrain (FSV) in Denver, Colorado, with 15 MWe. In contrast, the German Jülich Research Center built the AVR based on a pebble bed design using solid fuel containing thorium, uranium, and helium as coolants. In 1985, two decades later, AVR operated the Thorium High-Temperature Reactor (THTR-300). THTR generated 295 MWe operating with 675,000 balls of 6 cm diameter and helium as a coolant. Table 2 displays high-temperature helium reactors.

Table 2. Classification of high-temperature reactor designs using several fuels and arrangements.

Physical properties	Dragon	AVR	FSV	Peach Bottom	THTR-300
Operation	1966-1975	1969-1988	1979-1989	1967-1974	1983-1987
Power (MWth)	20	46	842	115	296
Fuel kernel	UO_2	UO_2-ThO_2	ThC	UCO	UO_2-ThO_2
Fuel coating	TRISO	TRISO	Carbide	TRISO	TRISO
Fuel arrangement	Prismatic	Pebble bed	Prismatic	Prismatic	Pebble-bed
Helium pressure (MPa)	2.0	1.1	4.8	2.	4.0

The HTGR operates at temperatures between 750 and 950 °C and employs graphite as a moderator. Two core types employed in HTGRs are prismatic blocks and spherical fuel using helium as a coolant. A pebble-bed high-temperature gas-cooled reactor (PB-HTGR) was the first design. The Pebble-Bed Fluoride-Salt-Cooled High-Temperature Reactor (PB-FHR) is the second one. The VHTRS and HTGRs implemented the thermochemical sulfur-iodine cycle at high temperatures of 950 °C. Table 3 depicts a comparison of the thermal parameters of high-temperature designs.

Table 3. High-temperature thermal designs FHR-PB, AHTR, MSR, PBMR, and the fast design MSFR.

Reactors Design	MK-1	MSFR	AHTR	MSR FUJI	PBMR
Power (MWth)/(MWe)	236/100	3000/1500	3400/1530	450/200	400/175
Fuel Material	TRISO/UCO	$^{233}UPuF_3$-ThF_4	1530	$^{233}UF_4$-ThF_4	UO_2
Coolant	$^{7}LiF\text{-}BeF_2$	$^{7}LiF\text{-}BeF_2$	$^{7}LiF\text{-}BeF_2$	$^{7}LiF\text{-}BeF_2$	Helium
Moderator	Graphite	-	Graphite	Graphite	Graphite
Inlet/outlet temperature (°C)	600-700	650-750	650-700	565-704	250-750
Power density (MWth/m^3)	22.7	48	12.9	7.3	4.0

Next-generation designs have proposed TRISO-coated particle fuels in several cases. Today, there are prototypes, such as the KP-FHR of Kairos Power, the Xe-100 (X-energy), and the eVinci of Westinghouse, adopting TRISO fuel. Features include operation at low pressure at high temperatures, as power densities ranging from 10 to 30 MW/m^3 are higher than those of modular helium reactors below 5 MW/m^3.

The TRISO fuel pebbles used in the FHR-PB and Mark-1 have a diameter of 3.0 cm, which is half that of the pebbles used in helium-cooled reactors. As a result, FHRs combine designs using pebbles made from carbon spheres and FLiBe as coolant (Scarlat et al., 2014). At atmospheric pressure, Mark-1 runs with a mass flow rate of 976 kg/s, a $^{7}LiF\text{-}BeF_2$ core inlet temperature of 600 °C, and a core outlet temperature of 700 °C. Mark-1 works on advanced Firebrick Resistance-Heated Energy Storage (FIRES) (Stack et al., 2019). FIRES is a thermal energy storage concept permitting power generation flexibility as a function of demand. Nuclear Air-Brayton Combined Cycle (NACC) and FIRES store heat power in ceramic firebricks (Qu et al., 2022).

Several MSRs operate on the thermal spectra, with fuel dissolved in the molten salt forming a liquid fuel. In the HTGR and FHR, the pebbles are coated with particle fuel using graphite as a moderator. Helium-cooled reactors permit an extended range of temperatures inside the pebble bed, from a 250 °C inlet temperature to 750 °C for the core outlet (Li et al., 2023).

2.2 Pyrocarbon layers of the pebble fuel

The TRISO fuel is practically indestructible and highly stable under regular operations and accident scenarios (Helmreich et al., 2022). The TRISO fuel can withstand all conditions for normal operations and accident scenarios because it is practically indestructible and highly stable under radiation (Helmreich et al., 2022). TRISO fuel contains five layers of pyrolytic carbon surrounding nuclear fuel cores. In the center, we have spherical fertile particles. Next, it has a low-density buffer layer surrounding the core and is a porous medium to absorb fission products.

The buffer layer is a container for fission products without transferring stress forces to the outer layers. Buffer layers show thicknesses of 85 µm to 94 µm with a low density of 1.0 g/cm^3 and contain about 50% void. The first pyrolytic carbon (PyC) layer has thicknesses ranging from 37 µm to 41 µm and densities around 1.9 g/cm3. The silicon carbide (SiC) layer showed thicknesses ranging from 36 µm to 51 µm. SIC provides structural support to avoid deformation under irradiation in the carbon layers. The outermost pyrolytic carbon (OPyC) layer has a thickness of 40 µm to protect the SiC during manufacturing. Figure 1 displays the coating layers used in spheric TRISO-coated particle fuel.

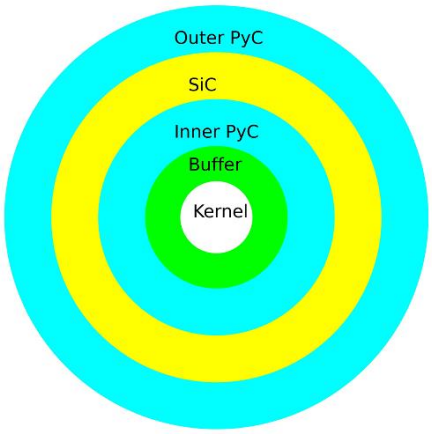

Figure 1. TRISO layers: kernel, Buffer, inner PyC, SiC, outer PyC.

The Advanced Gas Reactor Fuel Development and Qualification (AGR) program qualifies TRISO fuels until 2026 (Morris et al., 2018). The AGR plan shows the following phases: AGR-1, AGR-2, AGR-3/4, and scheduled for 2022–2026, phase AGR-5/6/7. Table 4 depicts the TRISO fuel properties of the pebble, kernel, and carbon layers.

Table 4. TRISO coated fuel used in Mark-1 compared with AGR plan and German of the1990s.

TISO fuel factors	**PB-FHR**	**HFR-P4**	**R2-K12**	**AGR-2**
Fuel kernel diameter (µm)	400	497	494	426.7
Fuel Kernel density (g/cm^3)	10.5	10.81	10.12	10.966
Fuel kernel composition (µm)	$UC_{1.5}O_{0.5}$	UO_2	$(Th\text{-}U)O_2$	UCO
Enrichment U-235 (%)	19.90	9.82	89.57	14.02
Buffer layer thickness (µm)	100	93	85	98.9
PyC inner layer thickness (µm)	35	37	39	40.4
SiC layer thickness (µm)	35	51	37	35.2
PyC outer layer thickness (µm)	35	38	39	43.4

3. RESULTS AND DISCUSSION

Combinations of fluoride salts exhibit both beneficial and harmful traits. The two crucial chemicals are lithium fluoride and beryllium fluoride. There are two isotopes of lithium: Li-6 and Li-7. However, Li-6 has an expressive thermal neutron cross-section. FLiBe has a low neutron absorption cross-section, and the beryllium content is chemically toxic. (Sohal et al., 2010). The lithium of FliBe must be enriched to the ^{7}Li isotope at 99.9%.

Core heat transport calculation requires dominance of its properties, including density, heat capacity, viscosity, thermal conductivity, and vapor pressure. Besides, fluoride coolants benefit from being immune to the effects of volatile

fission products generated by liquid or solid fuels. The primary circuit of the thermal reactor used in the initial studies requires graphite as a moderator. Since ^{7}LiF-BeF_2 delivers heat in a power cycle between 600 °C and 700 °C, its melting and boiling points are 459 °C and 1430 °C, respectively. Salt temperatures must be kept at a minimum of 550 °C to reduce the risk of freezing and at a maximum of 700 °C due to the material limitations of heat exchangers. It is not excessively high relative to the melting point at atmospheric pressure. Gas bubble release reduces fluoride salt densities in the temperature range of 670 °C to 750 °C (Gehin et al., 2016). Appropriated molten salts for FHRs show properties with good similarity. Figure 2 displays the density of liquid molten fluoride salts used as coolants and liquid fuels.

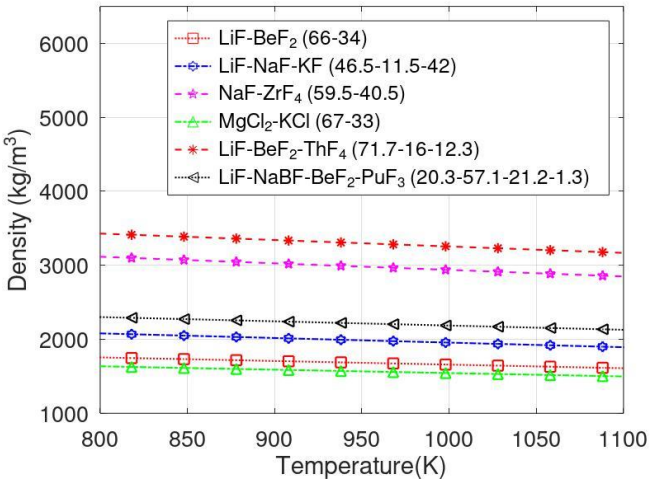

Figure 2. The density of liquid molten fluoride salts.

Following the formulation, ^{7}LiF-BeF_2 (66–34 mol%) has a sustained, temperature-independent liquid-state thermal conductivity of about 1.1 W/m·K. The thermal conductivity, on the other hand, declines and somewhat rises with temperature. The thermal conductivity of FliBe is slightly higher than that of FLiNaK, around 20%. Moreover, FLiNaK has a higher specific heat capacity than FliBe. Liquid metals, such as sodium and lead, show a little viscosity compared to molten fluoride salts. Figure 3 shows the dynamic viscosity of molten salts and dissolved fuels.

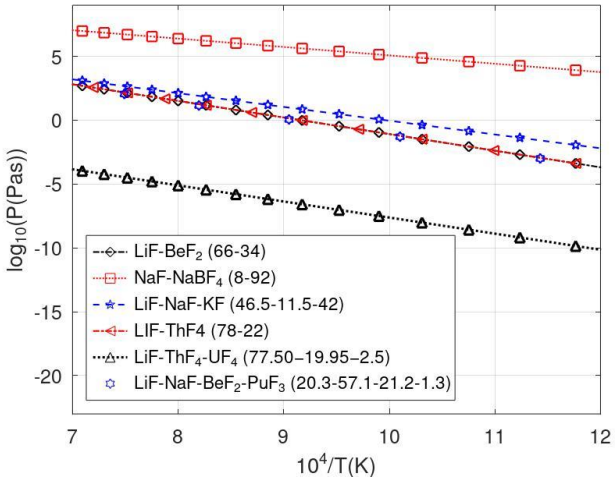

Figure 3. Dynamic viscosity of molten salts and dissolved fuels.

Since the 1950s, forced convective heat transfer experiments have initially focused on the ternary fluoride salt FLiNaK. To find the heat transfer coefficient, employ the Dittus-Boelter (DB) correlation with an accuracy of 15%. However, experiments for molten salts used an electrically heated Inconel tube with a Reynolds number of 2000 to 20000. The molten salts FLIBE and FLiNaK exhibit several notable thermodynamic properties, including low pressure and high heat capacity, a high boiling point, satisfactory viscosity, and a suitable Prandtl number.

There is good agreement with the Sieder-Tate correlation found for LiF–BeF_2–ThF_2–UF_4 and $NaBF_4$–NaF in the turbulent region at Reynolds above 15000. Figure 4 depicts the Prandtl number in the temperature function used to calculate the convection heat transfer coefficient.

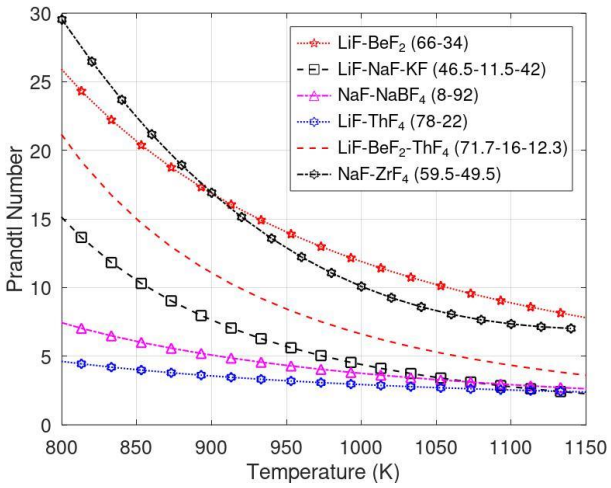

Figure 4. Prandtl number as a function of temperature at near atmospheric pressure

For many other designs, such as LWRs, micro-reactors, nuclear thermal propulsion, and salt-cooled reactors, the option TRISO is possible. TRISO kernels have included thorium carbide (ThC_2), thorium dioxide (ThO_2), plutonium dioxide (PuO_2), uranium dioxide (UO_2), and uranium oxycarbide (UCO), with diameters ranging from 100 µm to 500 µm and an enrichment of 19.74% U-235. TRISO fuels are structurally more resistant to extreme temperatures, corrosion, oxidation, and neutron irradiation than standard fuels, improving their fuel performance. Figure 5 shows the thermal conductivity of TRISO-coated layers.

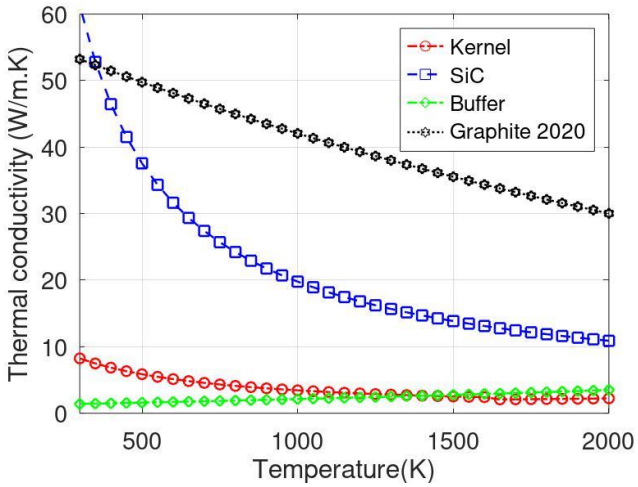

Figure 5. Temperature dependence of thermal conductivity for TRISO coatings.

TRISO fuels are structurally more resistant to extreme temperatures, corrosion, oxidation, and neutron irradiation than traditional reactor fuels, which impact fuel performance most. The buffer layer has a low density with a thickness of about 100 µm, producing a reservoir for fission gases such as Xe and Kr. Also, it must attenuate fission recoils and accommodate kernel swelling. The Mark-1 uses fuel pebbles with a diameter of 3.0 cm, which allows for more effective heat transmission thanks to salt cooling than helium cooling. Uranium oxicarbide (UCO) is a mixture of UO_2 and UC_2 in high-temperature gas reactors. Kernels containing UCO perform better than UO_2 and have a high safety margin. UCO creates CO through reactions between the carbon buffer and the extra oxygen released during fission. In contrast, the mixture of (UO_2-UC-UC_2) has multiple phases, which could reduce the internal gas pressure that causes TRISO failure.

The UCO kernel manufacturing route adopts the internal gelation process. Summarily, it combines internal gelation with carbothermal reduction. Phases comprise preparing the uranium solution, forming gelled microspheres, and sintering. There are differences in heat capacities between the pyrocarbon layers of TRISO fuels. Figure 6 depicts the heat capacities of TRISO coating layers. Figure 7 illustrates the thermal expansion coefficient of TRISO coating layers.

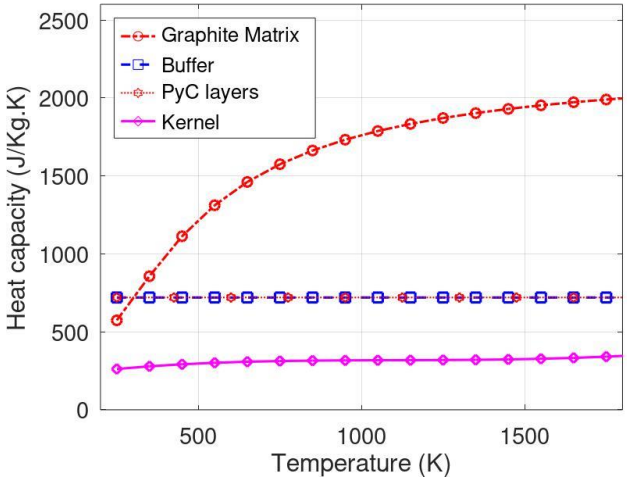

Figure 6. Heat capacity in function of the temperature of TRISO layers

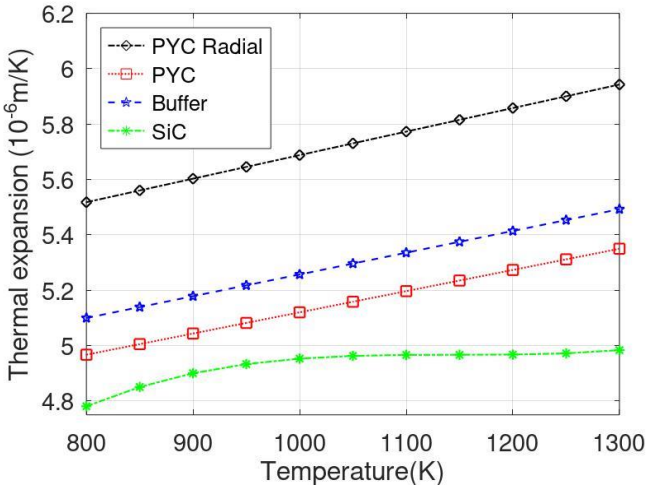

Figure 7. Thermal expansion coefficients of TRISO coatings.

3.1 Heat removal system of FHRs

A primary method of keeping nuclear reactors safe is using reliable methods to remove the decay heat. Thus, the FHR-safe system inherits three systems from other reactor designs, including decay heat removal. The first is the Direct Reactor Air Cooling System (DRACS) (Liu et al., 2018). In contrast, the Reactor Vessel Air Cooling System (RVACS) uses the natural air circulation through the reactor vessel to degrade heat, The third option is the silo cooling system (SCS) used for the decay heat removal system in a beyond-design accident. These tree heat removal systems aggregate sufficient capability to avoid catastrophic accidents.

Performance evaluation of decay heat removal systems for FHR resulted in three complementary concepts: DRACS, RVACS, and SCS. These systems are all built on technology initially created for other types of reactors. However, sodium shows a lower heat capacity of 1.25 J/kgK at 673 K than FliBe, with 2369 J/kgK. However, FliBe has a high volumetric heat capacity that forces mechanical adaptations, including the size of the heat exchangers, internal piping, valves, and internal components.

The DRACS has three coupled loops operating through natural circulation and convection. The DRACS Heat Exchanger (DHX) and the Natural Draft Heat Exchanger (NDHX) are the two heat exchangers that connect these loops. The fluidic diode reduces parasitic flow into the DRACS primary loop. Under accident scenarios, the DRACS is prepared for activation. DRACS transfers heat to a thermosiphon-cooled or natural heat exchanger that rejects heat from ambient air, which serves as the ultimate decay heat sink. Figure 8 depicts the half-PB-FHR Mark-1 core design, operating with a DRACS heat exchanger and fluid diode.

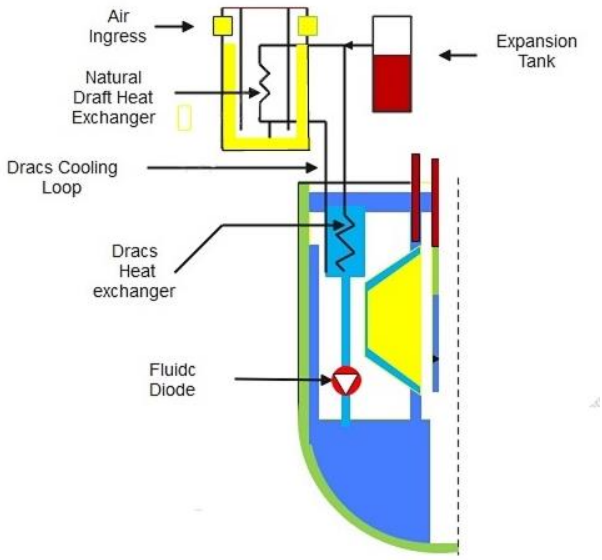

Figure 8. The Direct Reactor Auxiliary Cooling System is a passive heat removal system in FHRs.

The thermal conductivity value of 1.0 W/mK used for FLiBe heat capacity is 2390 J/kgK. While for the FLINaK, it is 0.92 W/m·K and 1940 J/kg·K. The packing factor adopted for FHR Mark-1 is 0.60, and the coolant velocity is around two m/s for both options, FLiBe and FLiNaK. Equations (1), (2), and (3) depict FLiBe properties given as a temperature function in K.

$$\rho_{FLiBe} = 2413.27 + 0.048T \quad (1)$$

$$\mu_{FLiBe} = 4638 \times 10^5 / T^{2.79} \quad (2)$$

$$k_{FLiBe} = 0.7662 + 0.0005T \quad (3)$$

where μ is the dynamic viscosity in kg/ms, ρ is the density in kg/m^3, and T is the temperature in K.

In FHR, the core average Reynolds number is over 1250, and the core average Prandtl number is 18.42. The average effective thermal conductivity of a TRISO sphere is around 15 W/mK. They composed spheres of TRISO fuel with a spherical fuel kernel and four coating layers: a porous carbon buffer layer, an IPyC layer, a SiC layer, and an OPyC layer. Mark 1's core contains around 470,000 fueled pebbles and 218,000 unfueled pebbles. One pebble produces 500 watts. Each pebble contains 1.5 g of uranium enriched at 19.9%, showing an external area of 0.00282 m^2 with an estimated core heat flux of 0.189 MWth/m^2. Equations (4), (5), (6), and (7) depict how it can calculate the convection heat transfer of the FHR core.

$$Nu = Pr^{1/3} \left[(1.18\, Re^{0.58})^4 + (0.23\, Re^{0.75})^4 \right]^{0.25} \quad (4)$$

$$Re = \rho V_s d_{pebble} / \mu P_f \quad (5)$$

$$\mathrm{Pr} = \mu \mathrm{Cp} / \mathrm{k} \quad (6)$$

$$h = kNu / d_{pebble} \quad (7)$$

where μ is the dynamic viscosity in (Pas), *Pf* is the packing factor of 0.6, *Vs* is the coolant velocity in m/s, *Pr* signifies the Prandtl number, *Re* represents the Reynolds number, and *k* is thermal conductivity (W/mk).

The active volume of fuel is 10.4 m^3, with a power density of 22.7 MWth/m^3, resulting in 236 MWth. The nominal coolant flow rate in the Mk1 design is 0.54 m^3/s, which uses approximately 47 m^3 (91,970 kg) of FliBe as its main salt. Many pebble bed codes are used to calculate the coolant temperature throughout the reactor and the fuel temperature, using the coolant temperature as a boundary condition. The fuel performance code PARFUME calculates the mechanical response of the pebble-bed spherical fuels under irradiation. Figure 9 shows the convection heat transfer of PB-FHR using FliBe compared with FLiNaK.

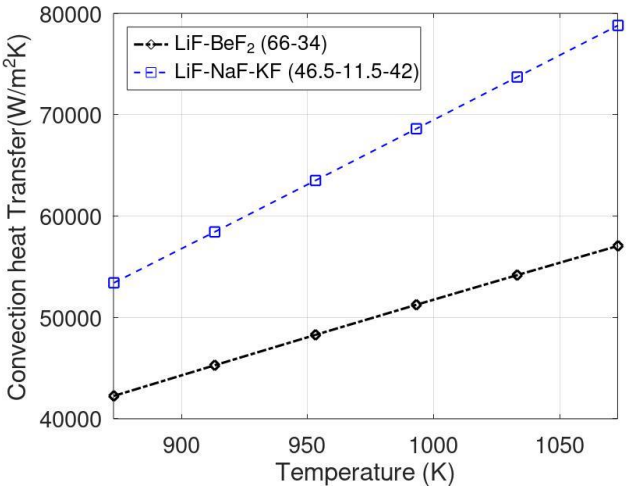

Figure 9. Convection heat transfer for FliBe and FLiNaK

4. CONCLUSION

One of the main advantages of nuclear liquid fuels based on molten salts is that they may provide online processing of fission products. The technique most commonly employed for removing fission products is reductive extraction, which removes uranium fuel before the fission products. Using molten salts in high-temperature reactors operating near atmospheric pressures is advantageous over helium-gas-cooled reactors. The features of the molten salt FliBe include its low melting point of 459 °C, high boiling point, and thermal conductivity of 1.1 W/mK. In addition, it shows a low vapor pressure of 1.2 mmHg at 900 °C and a high specific heat capacity of 2390 J/kgK, supporting the use of this material. Fluoride molten salt showed a high Prandtl number of 10 to 20. This way, FliBe, FLiNaK, and NaF-ZrF_4 coolants meet better specifications. The high density of these salts in the liquid state and their high volumetric capacity are positive factors, enabling more compact nuclei. They use encapsulated, coated particles in TRISO fuel with a power of 500 W per sphere of 3 cm diameter. The FHR Mark-1's operating parameters in the thermal spectrum are between 600 °C and 700 °C. The expertise accumulated over the years in Germany for helium-cooled reactors with a diameter of 6 cm and spherical fuels has made substantial progress. NACC cycles use a GE7 gas turbine to improve the thermal efficiency of FHRs to 66%.

5. ACKNOWLEDGEMENTS

The author expresses profound appreciation to the Energy and Nuclear Research Institute and the National Nuclear Energy Commission (IPEN/CNEN-SP) for their technological help in making the study presented here possible.

6. REFERENCES

Blandford, E., Brumback, K., Fick, L., Gerardi, C., Haugh, B., Hillstrom, E., and Zweibaum, N.,2020. Kairos power thermal hydraulics research and development. Nuclear Engineering and Design, vol. 364, pp. 110636.

Carrara, S., 2020. Reactor ageing and phase-out policies: global and regional prospects for nuclear power generation. Energy Policy, Vol. 147, pp.111834.

Cousse, J., 2021. Still in love with solar energy? Installation size, affect, and the social acceptance of renewable energy technologies. Renewable and Sustainable Energy Reviews, Vol. 145, pp. 111107.

Elder, R., and Allen, R., 2009. Nuclear heat for hydrogen production: Coupling a very high/high-temperature reactor to a hydrogen production plant. Progress in Nuclear Energy, Vol. 51(3), pp. 500–52.

Fernández-Arias, P., Vergara, D., and Orosa, J. A., 2020. A global review of PWR nuclear power plants. Applied Sciences, vol. 10(13), pp. 4434.

Forsberg, C., Wang, D., Shwageraus, E., Mays, B., Parks, G., Coyle, C., and Liu, M., 2019. Fluoride-salt-cooled high-temperature reactor (FHR) using British advanced gas-cooled reactor (AGR) refueling technology and decay heat removal systems that prevent salt freezing.

Haubenreich, Paul N., and J. R. Engel., 1970. Experience with the molten-salt reactor experiment. Nuclear Applications and Technology vol 8.2, pp: 118–136.

Helmreich, G. W., Kercher, A. K., Gerczak, T. J., Richardson, D., Montgomery, F. C., Skitt, D. J., and Hunn, J. D., 2022. Microstructure of irradiated AGR TRISO particle buffer layers as measured by X-ray computed tomography. Journal of Nuclear Materials, vol. 572, pp. 154061

Ho, M., Obbard, E., Burr, P. A., and Yeoh, G., 2019. A review on the development of nuclear power reactors. Energy Procedia, vol. 160, pp. 459–466.

Krey, V., Luderer, G., Clarke, L., and Kriegler, E., 2014. Getting from here to there–energy technology transformation pathways in the EMF27 scenarios. Climatic change, vol. 123, pp. 369-382.

Li, X., Zhang, D., Yun, S., Zhou, X., Jiang, D., Lv, X., and Liu, X., 2023. Design and optimal thermal efficiency contrastive analysis on closed Brayton cycle systems with different fluids of fluoride-salt-cooled high-temperature advanced reactor. Applied Thermal Engineering, vol. 226, pp. 120291.

Liu, M., Hughes, J., Ali, A., and Blandford, E., 2018. Conceptual design of a freeze-tolerant Direct Reactor Auxiliary Cooling System for Fluoride-salt-cooled High-temperature Reactors. Nuclear Engineering and Design, vol. 335, pp. 54–70.

MacPherson, H. G. 1985. The molten salt reactor adventure. Nuclear Science and Engineering, vol. 90.4, pp: 374–380.

Morris, R. N., Hunn, J. D., Baldwin, C. A., Montgomery, F. C., Gerczak, T. J., and Demkowicz, P. A., 2018. Initial results from safety testing of US AGR-2 irradiation test fuel. Nuclear Engineering and Design, vol. 329, pp. 124–133.

Novak, A. J., Schunert, S., Carlsen, R. W., Balestra, P., Slaybaugh, R. N., and Martineau, R. C., 2021. Multiscale thermal-hydraulic modeling of the pebble-bed fluoride-salt-cooled high-temperature reactor. Annals of Nuclear Energy, vol. 154, pp. 107968.

Pioro, I. L., Duffey, R. B., Kirillov, P. L., Fialko, N. M., and Pioro, R. M., 2023. *Current status and future trends in the world nuclear-power industry. Handbook of Generation IV Nuclear Reactors*, pp. 85–108.

Qu, X., Yang, X., and Wang, J., 2022. Characteristics Analysis of Combined Cycle Coupled with High-Temperature Gas-Cooled Reactor Based on Progressive Optimization. Frontiers in Energy Research, vol. 9, pp. 1011.

Reitsma, F., Strydom, G., De Haas, J. B. M., Ivanov, K., Tyobeka, B., Mphahlele, R., Sikik, U. E., 2006. The PBMR steady-state and coupled kinetics core thermal-hydraulics benchmark test problems. Nuclear Engineering and Design, vol. 236(5-6), pp. 657–668.

Satvat, N., Sarikurt, F., Johnson, K., Kolaja, I., Fratoni, M., Haugh, B., and Blandford, E., 2021. Neutronics, thermal-hydraulics, and multi-physics benchmark models for a generic pebble-bed fluoride-salt-cooled high-temperature reactor (FHR). Nuclear Engineering and Design, vol. 384, pp. 111461.

Scarlat, R. O., Laufer, M. R., Blandford, E. D., Zweibaum, N., Krumwiede, D. L., Cisneros, A. T., and Peterson, P. F., 2014. Design, and licensing strategies for the fluoride-salt-cooled, high-temperature reactor (FHR) technology. Progress in Nuclear Energy, vol. 77, pp. 406–420.

Schulenberg, T., 2022. Molten Salt Reactors. In The fourth generation of nuclear reactors: Fundamentals, Types, and Benefits Explained (pp. 147–165). Berlin, Heidelberg: Springer Berlin Heidelberg.

Seifried, J. E., Scarlat, R. O., Peterson, P. F., and Greenspan, E., 2019. A general approach for determination of acceptable FLiBe impurity concentrations in Fluoride-Salt Cooled High-Temperature Reactors (FHRs). Nuclear Engineering and Design, vol. 343, pp. 85–95.

Serp, J., Allibert, M., Beneš, O., Delpech, S., Feynberg, O., Ghetta, V., and Zhimin, D., 2014. The molten salt reactor (MSR) in generation IV: overview and perspectives. Progress in Nuclear Energy, vol. 77, pp. 308–319.

Singh, V., Wheeler, A. M., Lish, M. R., Chvala, O., and Upadhyaya, B. R., 2018. Nonlinear dynamic model of Molten-Salt Reactor Experiment, Validation, and operational analysis. Annals of Nuclear Energy, vol. 113, pp. 177–193.

Stack, D. C., Curtis, D., and Forsberg, C., 2019. Performance of firebrick resistance-heated energy storage for industrial heat applications and round-trip electricity storage. Applied Energy, vol. 242, pp. 782–796.

Suh, R., Martinson, S., Boldon, L., Breshears, A., and Therios, I., 2022. “Safeguards Considerations for Coated Particle Fuel Fabrication Facilities” (No. ANL/SSS-21/8), Argonne National Lab. (ANL), Argonne, IL (United States).

Vitart, X., Le Duigou, A., and Carles, P., 2006. Hydrogen production using the sulfur iodine cycle coupled to a VHTR: an overview. Energy conversion and management, vol. 47(17), pp. 2740–2747.

Wang, Q., Liu, C., Luo, R., Li, X., Li, D., and Macian-Juan, R., 2021. Thermo-economic analysis and optimization of the very high temperature gas-cooled reactor-based nuclear hydrogen production system using copper-chlorine cycle. International Journal of Hydrogen Energy, vol. 46(62), pp. 31563–31585.

Xu et al., 2019. Characterization of molten ^{7}LiF-BeF_2 salt impregnated into graphite matrix of fuel elements for thorium molten salt reactor. Nuclear Science and Techniques, vol 30(5). pp. 74.

Zohuri, B., 2020. *Generation IV nuclear reactors. In Nuclear Reactor Technology Development and Utilization*, Woodhead Publishing.

7. RESPONSIBILITY NOTICE

The author ensures that all responsibility for scientific information here is shown.